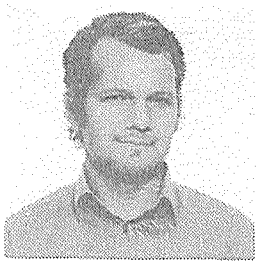

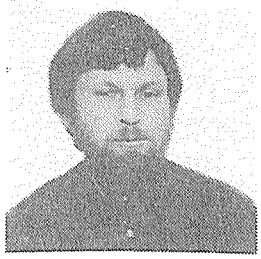

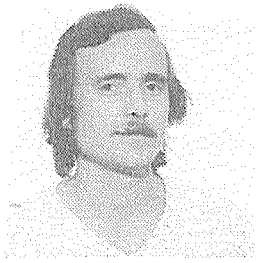

FINITE ELEMENT ANALYSIS OF PUNCHING SHEAR FAILURE OF REINFORCED CONCRETE SLABS

Dr.Ing. Svein Løseth
Siviling. Asbjørn Slåtto
Siviling. Tor G. Syvertsen

Research engineers at SINTEF (The Foundation of Scientific and Industrial Research at The Norwegian Institute of Technology)

The punching shear problem of reinforced concrete plates is studied by the use of a finite element program for nonlinear analysis of three-dimensional axisymmetric concrete structures. The importance of an accurate material model is demonstrated. Numerical results from the analyses are compared with experimental data.

Keywords: Punching shear, concrete plates, finite elements.

1. INTRODUCTION

Punching is a problem frequently encountered when reinforced concrete plates or shells are designed to sustain concentrated forces from column supports or external loads.
The punching problem is a very complex one, and a detailed analysis of the structural behaviour under a concentrated load requires accurate numerical models of the materials involved. Moreover, it is necessary to consider the stress and strain distributions through the thickness, so the problem becomes three-dimensional.

Simplified design rules for ultimate load calculations have been developed on an experimental and empirical basis /1,2,3/, and have proven very useful in ordinary design practice.
There are, however, many situations where these rules are insufficient and a more refined analysis is necessary.

Recent material models for reinforced concrete combined with the finite element method have demonstrated very good agreement between computed and observed behaviour of plate bending and similar types of problems /4,5,6/.

In spite of the brittle characteristics of concrete cracking, the overall structural behaviour of most concrete structures is rather ductile. In this report an attempt is made to use a finite element program for analysis of the rather brittle behaviour of punching shear failures of concrete slabs.

A full three-dimensional formulation of a problem of this kind would lead to very large equation systems, and the repetitive solutions would require a huge amount of computer resources. An axisymmetric description of the problem was judged to be sufficiently accurate, and as a program for such analyses was available /13/, this approach was chosen.

2. THE ANALYTICAL MODEL

2.1 The finite element model

The finite element method has proved to be a powerful tool in analysing nonlinear structural behaviour. For a given state of displacement, the strain field over the structure may be computed as well as stresses and nodal forces, R_{int}. The objective of the analysis is to find the state of deformation, characterized by the nodal point displacement vector r, where the internal forces balance the external load vector R:

$$R_{int} = R \qquad (1)$$

R_{int} is found by numerical integration of the internal stresses and computation of the equivalent nodal forces. Thus the accuracy of the solution will depend on how well the chosen material laws represent the true behaviour of the base materials.

Several material models for approximation of the multiaxial behaviour of concrete have been proposed in the literature. In this study one of the most accurate models, an improved version of the endochronic theory /7/, and a very simple elastic-ideally plastic model are employed.

2.2 Tensile cracking of concrete

Tensile cracking is one of the dominant nonlinear effects in concrete structures. In the present program this is accounted for by continuously checking the principal stresses at each integration point against the crack criteria defined by surfaces in the stress space as shown in Figure 1.

By this approach the development of every single crack can not be traced, but the effect of crack opening is present by a smeared representation.

The occurrence of a crack leads to an abrupt loss of concrete stiffness in a direction normal to the crack, as illustrated by the dashed line in the stress-strain diagram in Figure 2.

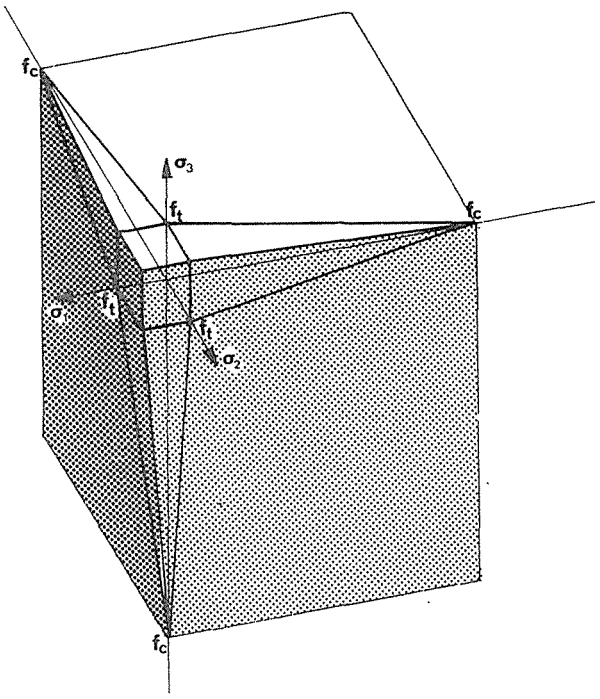

Figure 1 Tension cut-off criterion for stresses

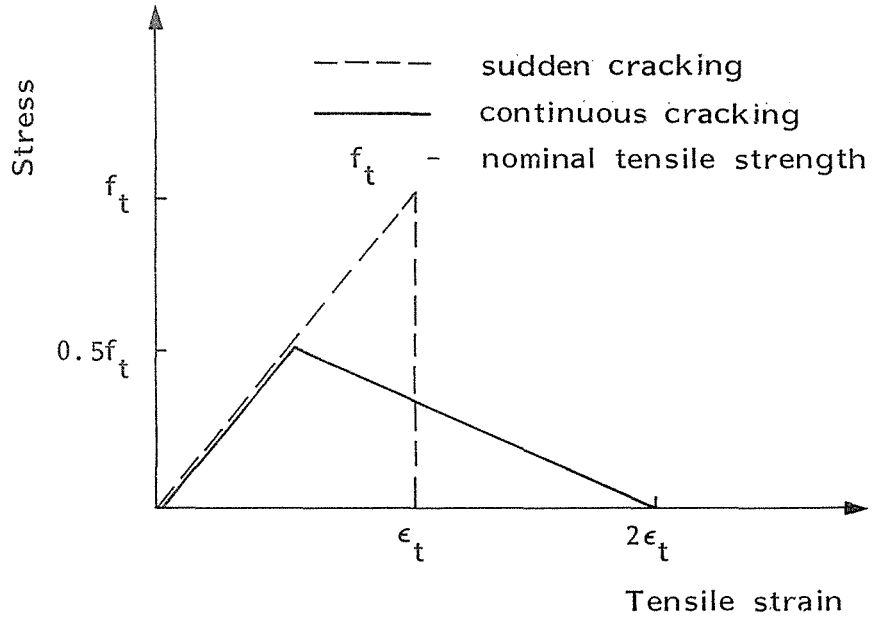

Figure 2 Uniaxial stress-strain curves in the tensile region

However, the use of this curve implies a sudden release of the total elastic energy stored in the region represented by the integration point. This does not represent the actual physical behaviour adequately. Moreover, in sensitive problems, as those in the present study, this formulation will very soon lead to numerical instabilities and breakdown of the algorithm. To avoid this problem, the stress-strain curve given by the solid line in Figure 2 is introduced. This curve simulates a more continuous movement of the crack tip thorugh the region of the integration point. Both curves represent the same amount of energy, but it is more smoothly released by the second and a more stable numerical algorithm is achieved.

2.3 Material models for concrete in compression

An accurate description of multiaxial stress-strain relationship of concrete is very complicated. So far, one of the best models for monotonic loading is the improved version of the endochronic theory. In this formulation the incremental constitutive relations, expressed by the deviatoric and volumetric components of stress (s_{ij},σ_v) and strain (ε_{ij},ε_v) are given by:

$$d\varepsilon_{ij} = \frac{1}{2G} ds_{ij} + s_{ij} d\zeta \qquad (2)$$

$$d\varepsilon_v = \frac{1}{3K} d\sigma_v + d\lambda + \sigma_v d\xi' + d\lambda' \qquad (3)$$

The first term on the right hand side of equations (2) and (3) are the elastic components, while the other terms represent inelastic contributions and are measures of accumulated damage. The internal variables ζ, λ, ξ' and λ' are expressed by hardening and softening functions that have been fitted to a large amount of experimental data /7/.

The endochronic theory gives good agreement with reported multiaxial stress tests, but as the algorithm for computation of stress increments is rather complex, it also requires relatively much computer time.

In many cases, however, the static response is totally dominated by the tensile cracking, and rude simplifications of the material law in compression can be justified. For this purpose an elastic-ideally plastic material model is incorporated in the program.

To examine the importance of the material model in compression for the class of problems treated in this study, these two extreme material models have been used in the analyses.

In Figure 3 the load-response curve for endochronic theory is compared to experimental data by Mills /8/. The curve from the

simple elasto-plastic model is shown for comparison. This curve does not change with variations in the confining pressure.

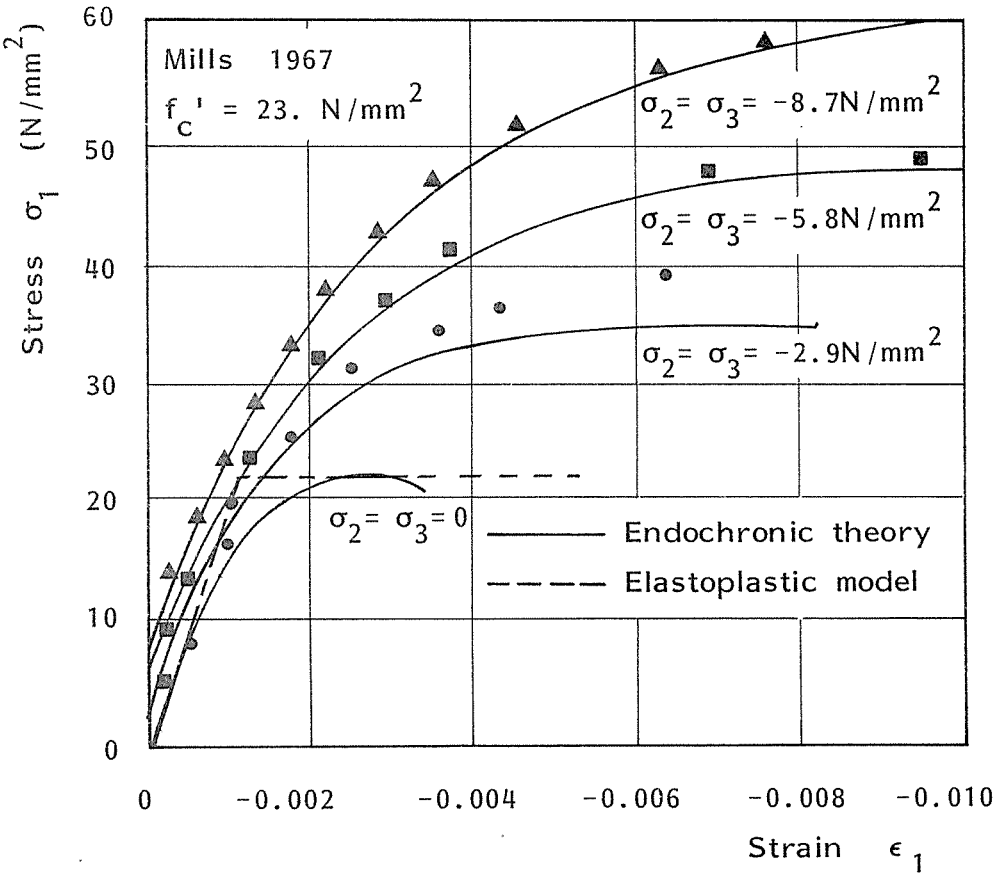

Figure 3 Comparison of material models to experiments with concrete in three dimensional states of stress

2.4 Modelling of reinforcement steel

Any element in the finite element model may be intersected by reinforcement layers. The layers may be arbitrarily located within the element, as shown in Figure 4. It is also possible to connect any two nodes with reinforcement bars.

The constitutive relations of the reinforcement steel is modelled by the mechanical sublayer technique. The basic idea of this method is to divide the steel cross section into a number of subareas, each with an elastic-ideally plastic material behaviour, but with different fictitious yield levels. The total stress is a weighed sum of the stresses in the sublayers.

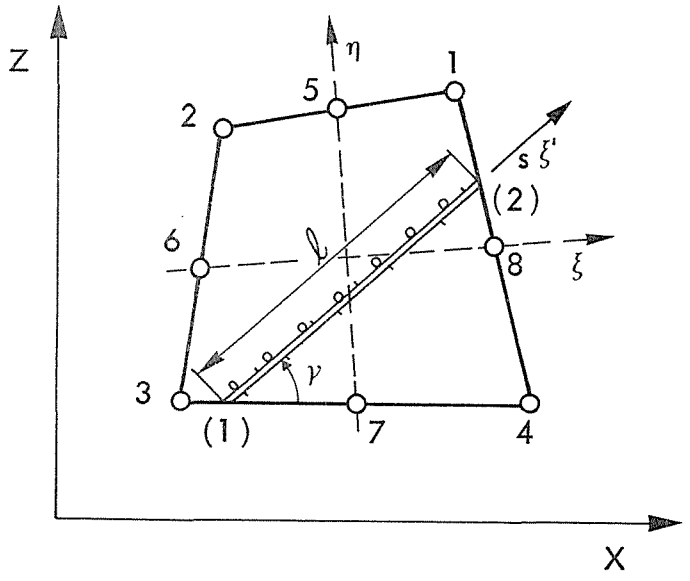

Figure 4 Reinforcement layers through an element

2.5 The Numerical Solution Method

The main purpose of the analysis is to determine the load-deflection curve of the structure, and in particular the ultimate load carrying capacity.

In order to be able to trace the deflections for increasing loads, an incremental loading procedure is chosen. Path dependence in the material constitutive laws and numerical stability problems in the solution process also necessitate this approach. A first approximation of the incremental nodal point deflection vector, Δr, may be found by:

$$K_T \cdot \Delta r = \Delta R \qquad (4)$$

where K_T is the structure's tangential stiffness matrix of the structure and ΔR the load increment.

As the material properties throughout the structure at the end of a load step is not known in advance, the equilibrium equation (1) is generally not satisfied. This calls for an iteration process where the unbalanced forces, R_u, found by

$$R_u = p \cdot R - R_{int} \qquad (5)$$

are applied at the right hand side of Equation (4). By accumulation of the displacements, and repeated use of Equations (4) and (5), the state of deformation that satisfies Equation (1) is found.

The parameter p in Equation (5) is a factor for scaling the external load level, such that the unbalanced forces can be minimized.

The value of p is determined by a procedure proposed by Bergan /9/. By this method the initial factorized stiffness matrix can be used throughout the analysis, and much computer time is saved. It is also possible to follow descending parts of the load-deflection curve without any special precautions. The method also opens for the possibility of displacement incrementation, i.e. the first displacement in an increment may be equal to previous increment multiplied by a scaling factor. The external load is scaled to minimize the unbalanced forces, and equilibrium iterations are performed in the ordinary way.
An automatic incrementation scheme included in the program soon appeared to be unreliable when applied to numerically sensitive problems like punching of concrete slabs, and it was necessary to introduce some kind of interactive control of the incrementation process. In this the user may optionally inspect some key parameters at the end of each increment, and decide whether it should be accepted or not. A rejected increment may be repeated with a new scaling factor decided on by the user.

2.6 Program input and output

Preparing input data to finite element programs may be a tedious job. This is to a great extent overcome by making an interface to the mesh generation program MGP /10/. The program itself contains a built-in module for generation of element reinforcement data.

Further, the output from nonlinear programs may be enormous. In the present program the amount of output may be selected by print and plot switches. The data may be stored on disk files, and the element mesh or the results may be graphically presented with the plotting programs FEM-PLOT /11/ and MATRIX-PLOT /12/.

3. NUMERICAL EXAMPLES

3.1 Description of specimens

Test cases for the numerical studies were selected from the well known experimental investigation by Kinnunen and Nylander /1/. Their tests were made on series of circular concrete slabs, supported at the center by column stubs and loaded uniformly along the circumference. The tests covered various types and amounts of flexural reinforcement, and different stub diameters.

Three of the specimens have been analysed in this study. Geometry and reinforcement spacing are shown in Figure 6. All the test cases have reinforcement in radial and ring directions, and conform to an axisymmetric model.

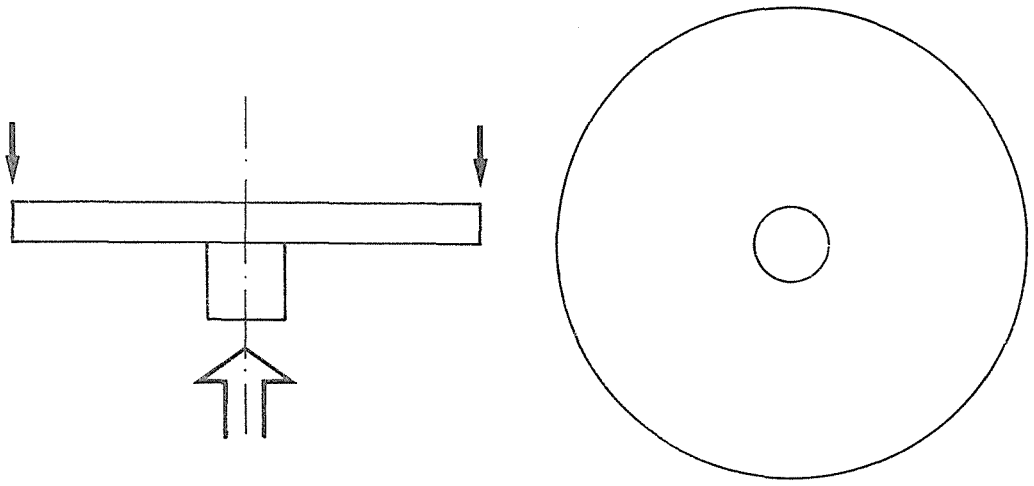

Figure 5 Principle for testing circular slabs

The reinforcement is Swedish Kam steel ribbed bars 12 mm in diameter. Test data are given in Table 1.

TABLE 1 : Test data

	Plate			
	IC15a	IC15b	IC30b	UNIT
Cube strength of concrete at 28 days	33.3	33.2	33.6	MPa
Yield point stress of steel	443	441	452	MPa
Mean effective thickness	126	124	130	mm
Observed ultimate load	198	285	429	kN
Observed flexural cracking load	70	110	134	kN
Observed shear cracking load	130	149	235	kN

The compressive strength as referred to a cylinder test was needed for the numerical model, and was taken to be 70% of the cube strength. The tensile strength was not reported by Kinnunen and Nylander, but has been estimated to be 10% of the cylinder strength.

3.2 Finite element meshes

The finite element models are shown in Figure 7. The element used is a 8-noded, isoparametric quadrilateral with 2 degrees of freedom at each node.

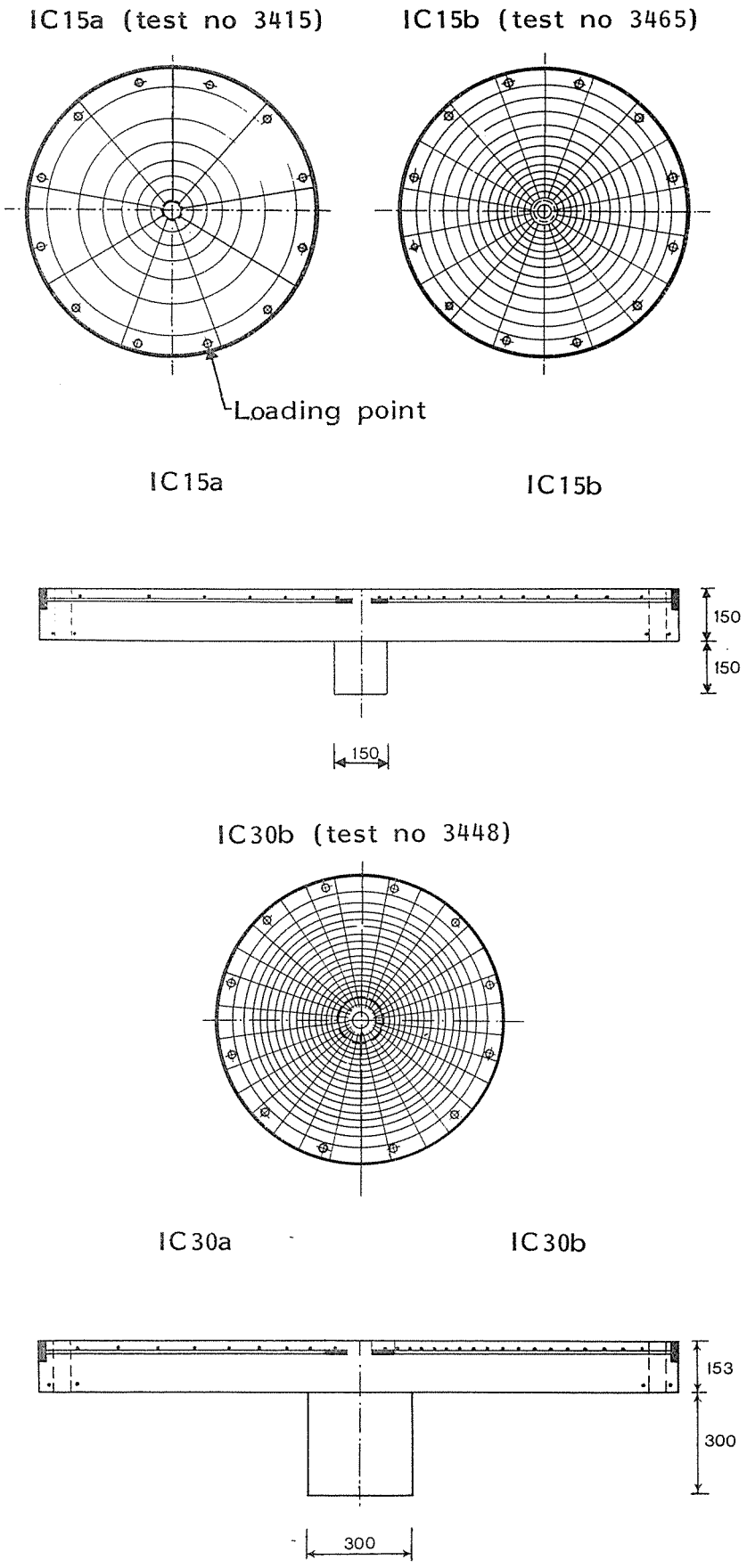

Figure 6 Geometry and reinforcement of the analysed plates

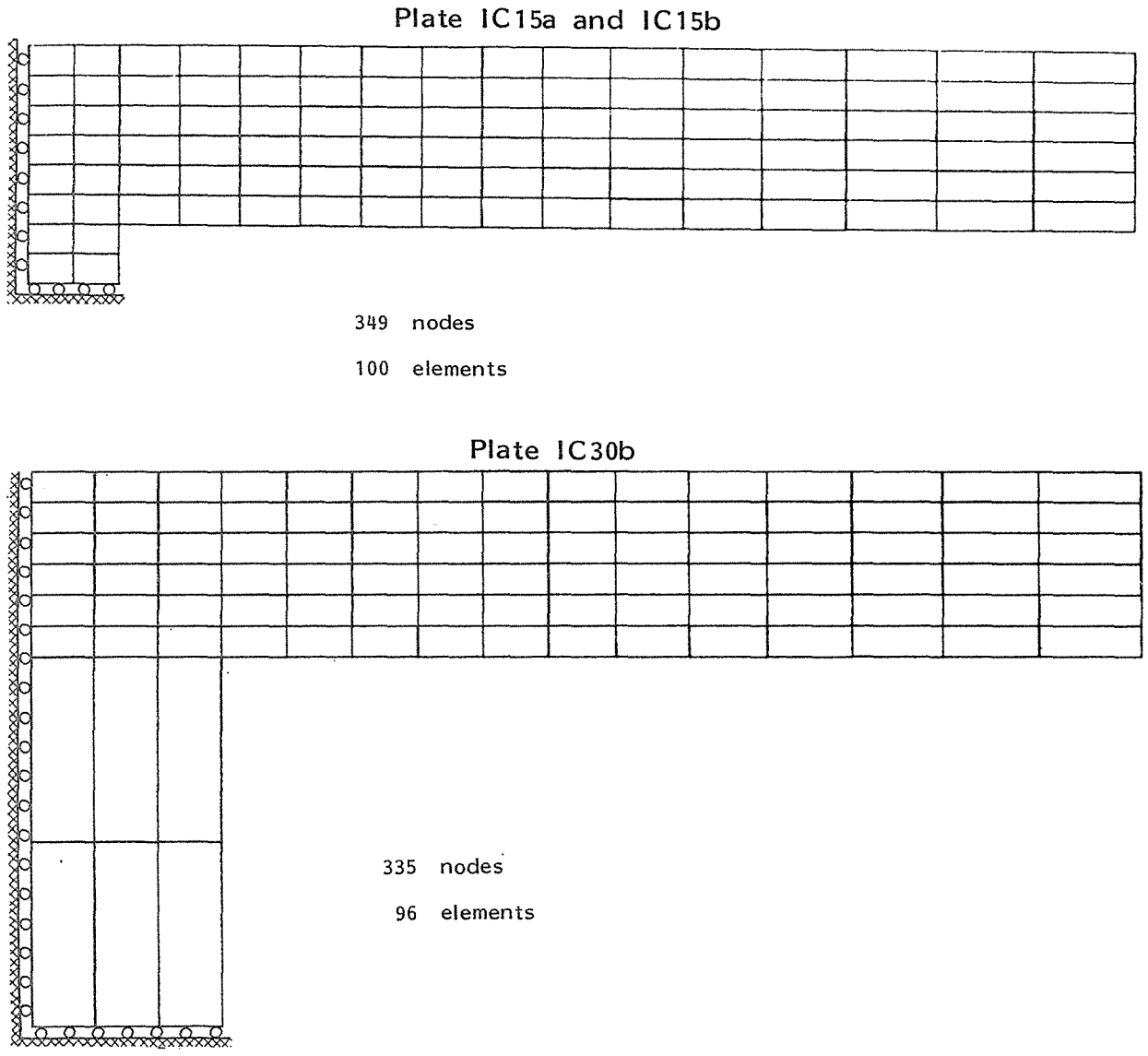

Figure 7 Finite element models

The reinforcement is modelled as two smeared layers located at the centerplane of the true reinforcement bars. The radial reinforcement has a constant total cross-sectional area, whereas the hoop reinforcements are approximated by a stepwise decrease in reinforcement area with increasing radius according to the bar spacing.

3.3 Computed results

Some parameter studies were performed with plate IC15b. Due mainly to the aggregate interlock, friction and dowel action of the reinforcement, some shear resistance remains in the concrete after cracking. This shear capacity may be accounted for by retaining a fraction of the original shear stiffness. To achieve this the shear modulus in the constitutive matrix is multiplied by a shear retention factor α, which normally is chosen in the range 0.0 - 0.5. The plate was analysed with two different values of the shear retention factor.

In Figure 8 the load-deflection curves from the two analyses are compared to the test results. In the first analysis, with a shear retention factor $\alpha = 0.5$, the ultimate load was calculated to be 305 kN (solid curve). In the second analysis the shear retention factor was 0.2, and the computed ultimate load was, in this case, 284 kN. In the test the load carrying capacity was measured to be 285 kN (dashed curve). The deviations between computed and observed ultimate load were thus 5% and -0.4%, respectively.

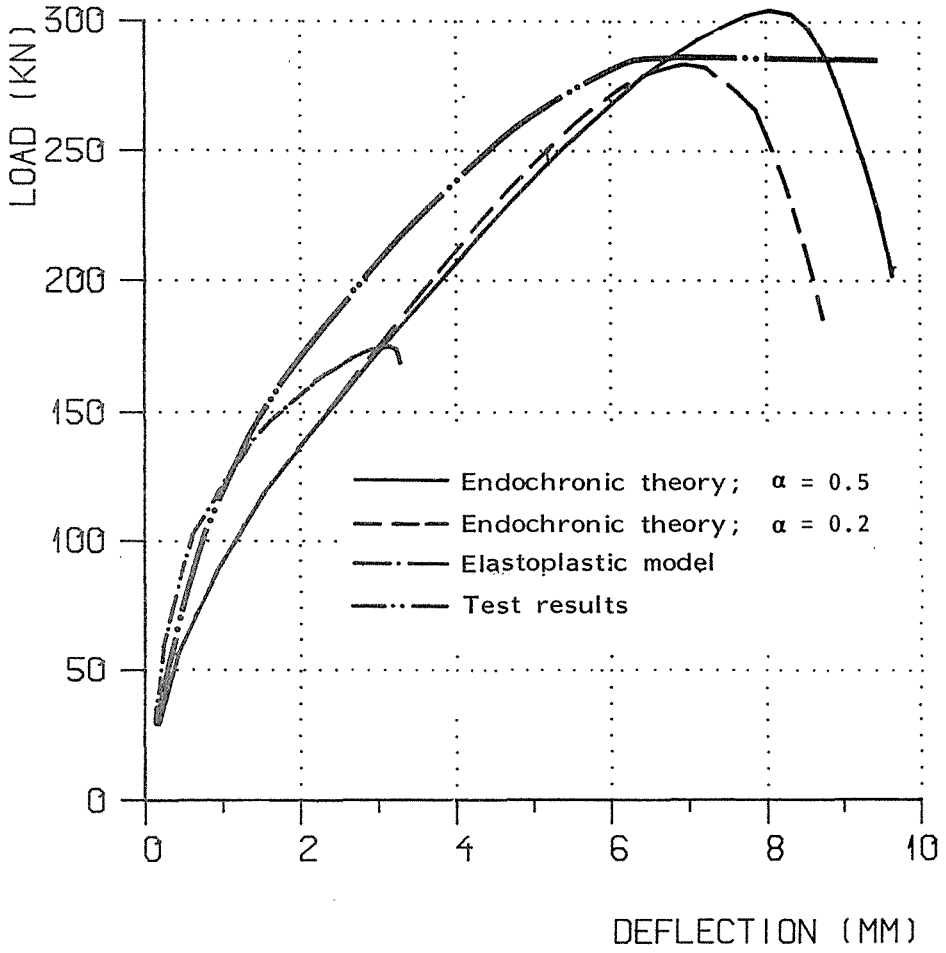

Figure 8 Plate IC15b. Computed and measured load deflection curves.

Since the shear retention factor 0.2 gave the best results, and also was on the safe side, this factor was used in all subsequent analyses.

The computed deflections are seen to be somewhat larger than the test curves. However, in the test only the rotation of the slab portion outside the shear crack was measured. The test curve has been computed by multiplying this rotation by the distance from the support to the loading point. This may account for some of the deviations as deformations near the support are not accounted for in the test curve.

The dash-dot curve in Figure 8 is the load-deflection curve for the same plate analysed with the elastic-ideally plastic material model. As illustrated in Figure 3 this model does not account for

higher strength with increasing confining pressure. This effect is of great importance in the punching shear mechanism. In Figure 9 the principal stresses just below ultimate load for the first analysis is shown. As could be expected stress concentrations occur near the support. Here the three-dimensional state of compression stresses give principal stresses well over the ultimate uniaxial compression strength.

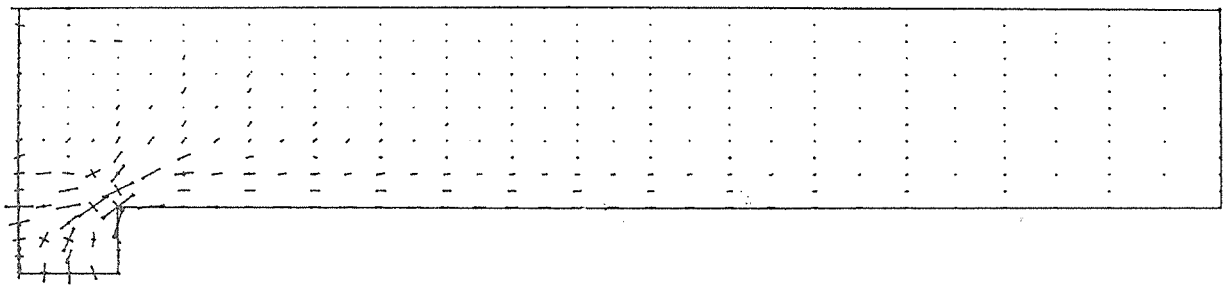

Figure 9 Principal stresses just below ultimate load. Endochronic theory $\alpha = 0.5$

Figure 10 shows the crack pattern and the extension of cracks for the ultimate load. In the row of elements next to the support, only one element remains uncracked. In the next load increment the hoop cracks penetrate through this element also, and the plate collapses. The typical fault mechanism of the plates is punching out a cone as indicated with the dash-doubledot line /1/. The computed crack directions coincide well with the observed fault line. This indicates that the correct sollapse mechanism has been found.

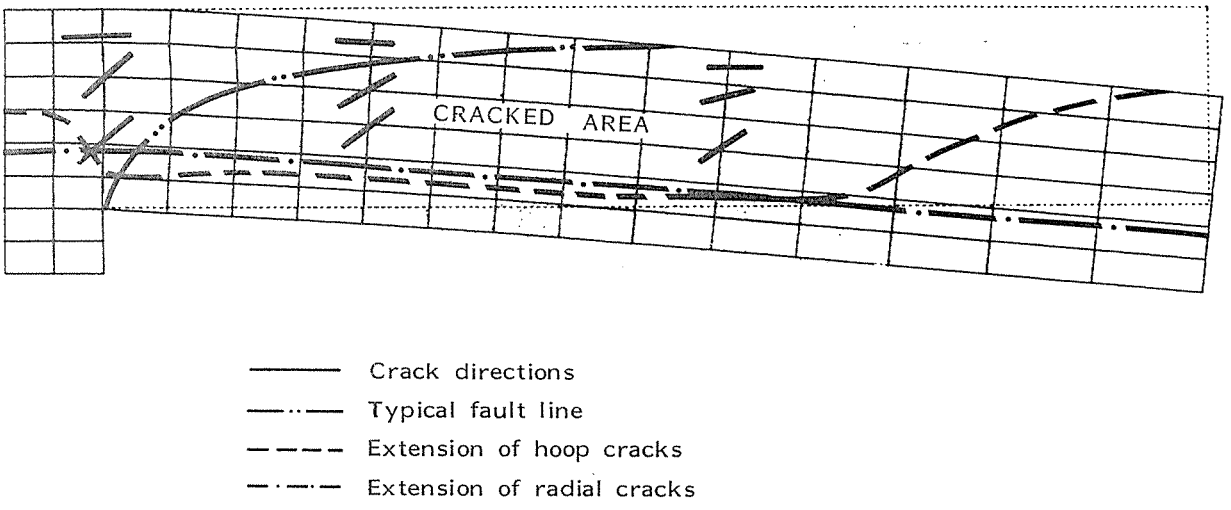

Figure 10 Deflection and crack pattern at ultimate load

Figure 10 also shows the computed deflections of the plate. The element near the support form a hinge mechanism, and combined with the radial slicing by cracks, the outer part almost forms a chain of rotating rigid bodies.

The overall stiffness of the structure may be measured by a parameter denoted the current stiffness parameter. In Figure 11 this parameter is plotted out for the three computer runs. The fast reduction in the stiffness at low loading is due to extensive cracking. At higher load levels the forming of new cracks almost stops, and further deformations mainly consists of straining and opening of the existing cracks. This is reflected by the almost flat platau of the curves in Figure 11. When the structure reaches the ultimate load, the stiffness drops below zero, and the deflections continue to increase even with a reduction in loading.

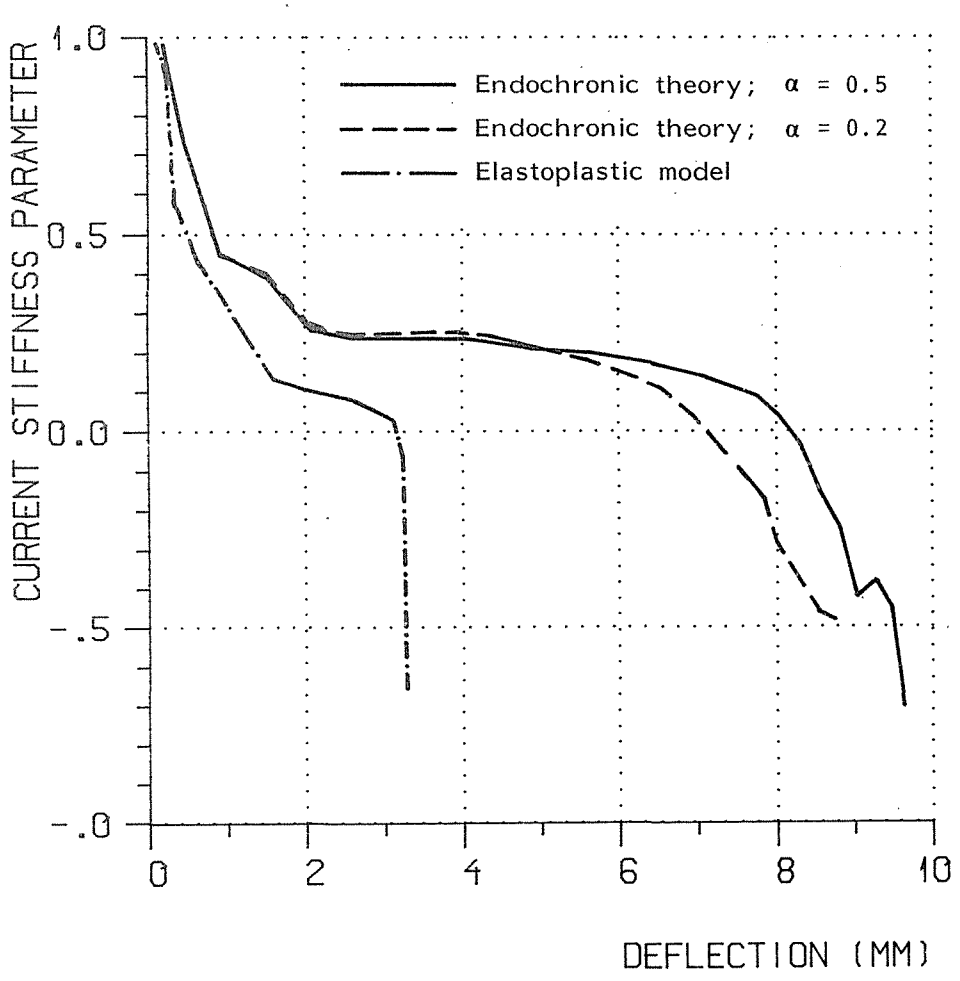

Figure 11 Stiffness reduction of plate

Plate IC15a had the same geometry as IC15b, but the reinforcement was reduced by 50%. Figure 12 shows the computed load-deflection curve for the plate.

In this case the testing resulted in a load carrying capacity of 198 kN. In the analysis a maximum of 236 kN was reached. At this level the plate had a sudden collapse, and the analysis method failed. As for the first plate, some divergence from the test deflections was found for this plate, but here the test gave larger deflections at higher load levels. For this plate an extensive cracking and abrupt loss of stiffness was found at a low level. See Figure 13.

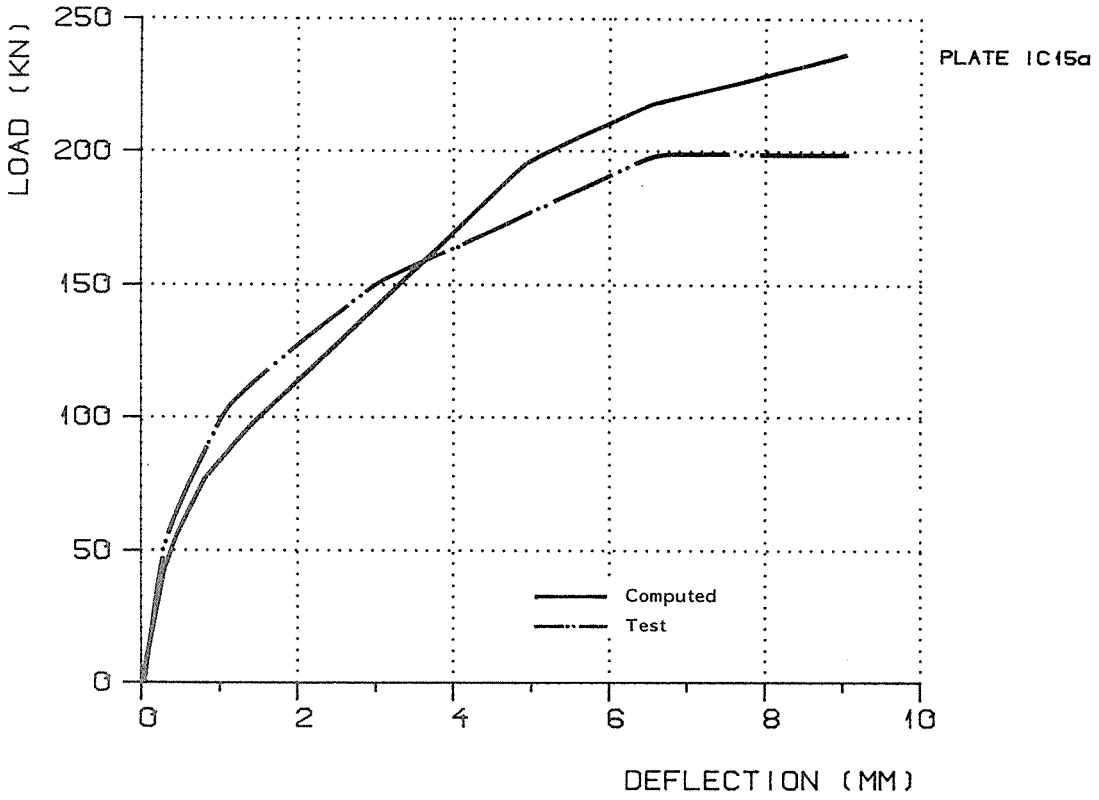

Figure 12 Load deflection curve for plate IC15a

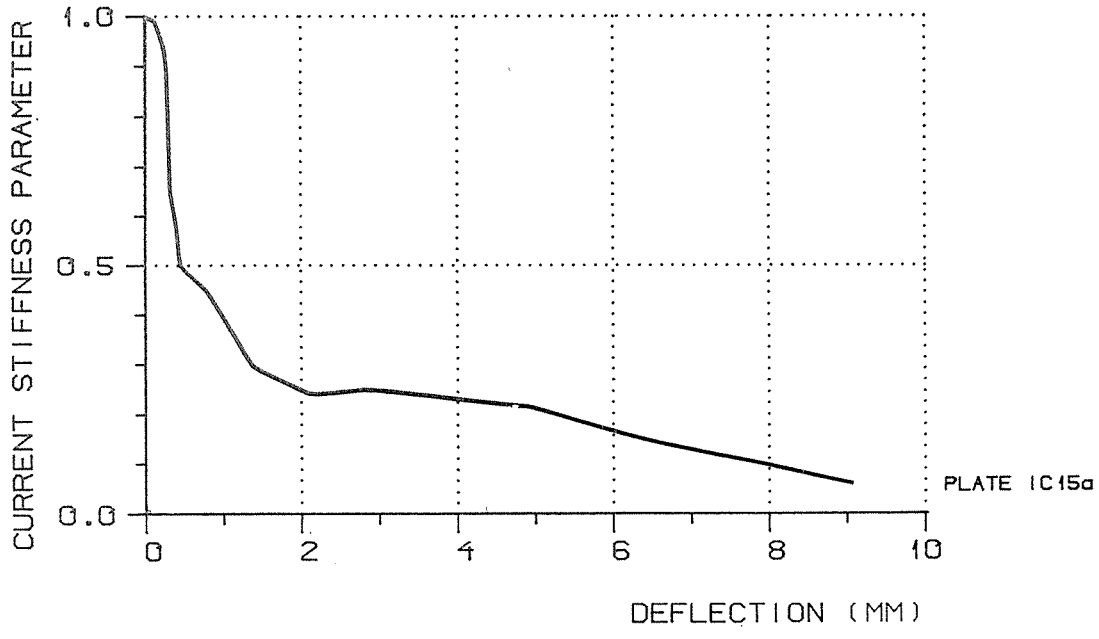

Figure 13 Current stiffness parameter for plate IC15a

This made the numerical algorithm unstable and led to a false collapse at low load levels in the first computer runs. However, by applying very small increments in this region the critical point could be passed, and the analysis then proceeded normally at higher load levels.

The third example, plate IC30b, had approximately 50% more reinforcement than plate IC15b. The diameter for the support column was 300 mm. In the test by Kinnunen and Nylander the ultimate load for this plate was found to be 429 kN, while our numerical model gave gave 470 kN. In Figure 14 the load-deflection curves for this plate are shown.

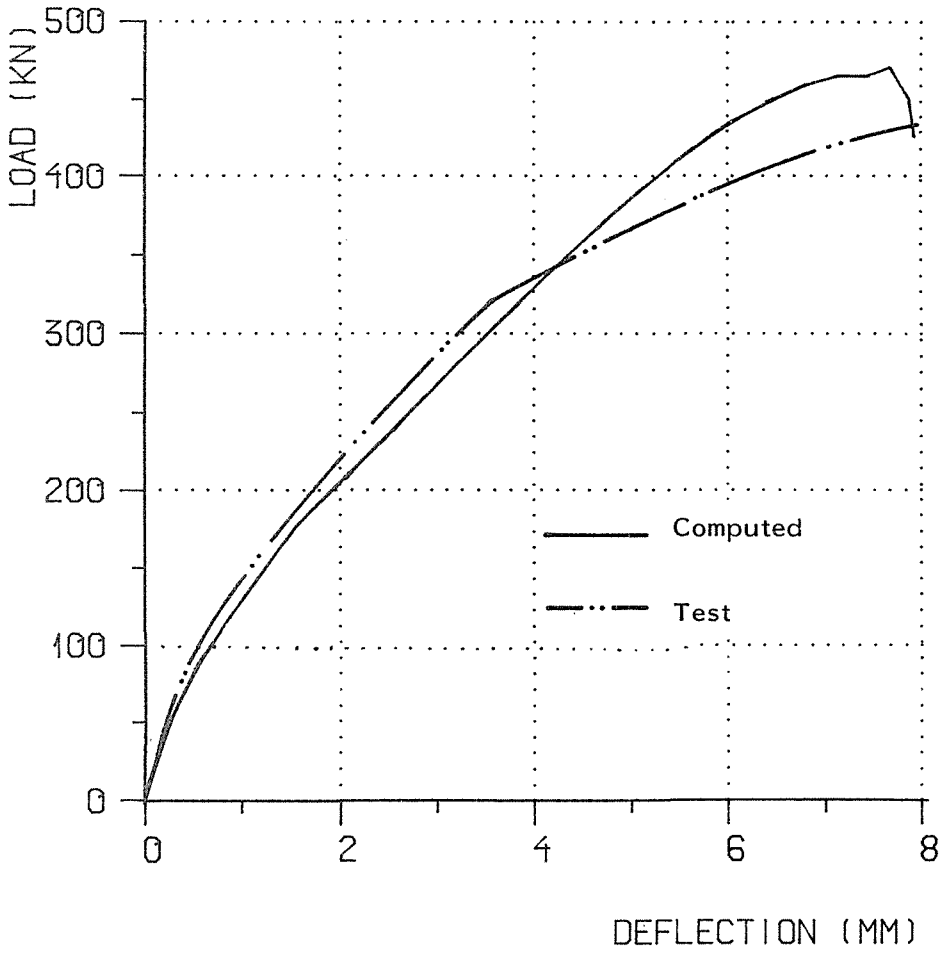

Figure 14 Load-deflection curve for plate IC30b

In the analysis this plate behaved in a much more ductile manner than had the other two, and no particular stability problems arose.

4. CONCLUSION

The study has shown that a finite element program for nonlinear analysis of concrete structures can be used for analysis of brittle problems such as punching of concrete slabs. However, the problem is so sensitive that one can not just select any non-linear program and expect successful analyses

Some of the experience gained during this study are summarized below.

* Abrupt stiffness cut-off when the stress reaches the tensile strength of the concrete at an integration point very soon leads to numerical instabilities. This an be avoided by a gradual stiffness reduction and a similar release of strain energy.
* It is important to have a material model for concrete that accounts for higher strength with increase in confining pressure. If not, concrete crushing will take place in critical regions at too low load levels.
* The program should possess interactive facilities that offer the user the option of program control during execution. Most important is the possibility to change the increment sizes, and to reject and recompute an increment that has not converged.
* In general, the ductility of a structure decreases with the amount of reinforcement, and there is reason to believe that some "brittleness limit" exists beyond which our approach cannot be used.
* Even with programs having the facilities mentioned above, numerical problems in the analyses must be expected. The analyses are rather time consuming, and studies like this may be expensive in terms of computer costs.

5. REFERENCES

/1/ Kinnunen, S. and Nylander, H.: 'Punching of Concrete Slabs Without Shear Reinforcement', *Kungliga Tekniska Högskolans Handlingar, Report No. 158*, Transactions of the Royal Institute of Technology, Stockholm, Sweden, 1960.

/2/ Scheidt, W., Ladner, M. und Rösli, A.: 'Berechnung von Flachdecken auf Durchstanzen', Beton-Verlag GmbH, Düsseldorf 1970.

/3/ "Skjærkraftkapasitet for plater med konsentrerte laster", Norsk Betongforenings Publikasjon nr. 6, Oslo 1978.

/4/ Sørensen, S.I.: 'Endochronic Theory in Nonlinear Finite Element Analysis of Reinforced Concrete', *Report No. 78-1*, Division of Structural Mechanics, The Norwegian Institute of Technology, The University of Trondheim, March 1978.

/5/ Arnesen, A.: 'Analysis of Reinforced Concrete Shells Considering Material and Geometric Nonlinearities', *Report No. 79-1*, Division of Structural Mechanics, The Norwegian Institute of Technology, The University of Trondheim, July 1979.

/6/ Løseth, S.: 'Nonlinear Analysis of Axisymmetric Reinforced Concrete Structures', *Report No. 82-1*, Division of Structural Mechanics, The Norwegian Institute of Technology, The University of Trondheim, April 1982.

/7/ Bazant, Z.P. and Shieh, C.L.: 'Endochronic Model for Nonlinear Triaxial Behaviour of Concrete' *Nuclear Engineering and Design* 47, 1978, pp 305-315. *Errata, Nuclear Engineering and Design* 51, 1979, p 309.

/8/ Mills, L.L.: 'A Study of the Strength of Concrete under Combined Compressive Loads', *Ph.D. Dissertation*, New Mexico State University, Las Cruces, December 1967.

/9/ Bergan, P.G.: 'Solution by Iteration in Displacement and Load Spaces', *Proceedings of the Europe-U.S. Workshop*, Ruhr-Universität Bochum, Germany, July 1980, pp 553-571.

/10/ Løseth, S.: 'MGP', *Institutt for statikk, NTH*, Trondheim October 1979.

/11/ Larsen, J., Aas, J. and Syvertsen, T.G.: 'FEM-PLOT - User's Manual' *SINTEF Report No. STF71 A81007*, Trondheim, July 1981.

/12/ Løseth, A.: 'MATRIX-PLOT', *Institutt for statikk, NTH*, Trondheim 1980.

/13/ Løseth, S.: 'CONAX MANUAL' *Institutt for statikk, NTH*, Trondheim, September 1982.